

# Free rotation of conducting and dielectric spheres in a uniform electrostatic field

A. Duviryak

Institute for Condensed Matter Physics of NAS of Ukraine,  
1 Svientsitskii Street, Lviv, UA-79011, Ukraine  
Tel.: +380 322 701496, Fax: +380 322 761158  
duviryak@icmp.lviv.ua

## Abstract

Rotation of conducting and dielectric spherical particles levitating in the uniform electrostatic field is considered. A dipole moment of the spherical particle induced by the external uniform electrostatic field is inclined to the field if the particle rotates. This causes the torque braking the rotation. Vectors of dipole moment and torque depend both on an angular velocity of the particle and its electric properties. Equations of rotary motion of the particle levitating in the external field are integrable in quadratures. Few examples of the conducting and dielectric particles are solved explicitly.

**Key words:** spherical particle, dipole moment, rotational dynamics

## 1 Introduction

A uniform electrostatic field induces in a motionless spherical conducting or dielectric particle a dipole moment which is parallel or antiparallel to the field. If the particle is immersed in a conducting fluid, the interaction of the field with the induced dipole moment may cause spontaneous rotation of the particle, known as the Quincke effect [1,2]. On the contrary, if the particle is already rotating in a vacuum or a non-conducting medium, the induced dipole moment becomes inclined to the field [3] and gives rise to the torque braking the particle rotation. The magnitude and the direction of the induced dipole moment depend on the angular velocity of the particle as well as on its electric properties. The same is concerned with the induced torque braking the rotation. Nowadays, nanoparticles in optical traps can be spun up to GHz, and the rotary frequency is in rapid progress [4–6]. The question arises naturally: may the aforementioned effects become essential in future experiments?

Here the rotation of neutral spherical particles levitating in the uniform electrostatic field under the action of the induced braking torque is analyzed. Both the conductive and dielectric particles are considered in Sections 2 and 3, respectively. The study is two-stage. On the first stage the electrostatic potential of a rotating particle and a corresponding induced dipole moment is calculated. This task requires a generalization

in Subsections 2.1–2.3 of results presented by T.B. Jones [2, 3] to the case where the axis of particle rotation is oriented arbitrarily with respect to the external field. Besides, the dispersion of dielectric permittivity must be taken into account in Subsection 3.1 when considering dielectric particles. On the second stage expressions for the torque of a dipole interaction with the external field is used to formulate and analyze the equations of rotary motion. They are shown integrable in quadratures for both conductive and dielectric particles; see Subsections 2.4 and 3.2, respectively. Few basic examples has been solved analytically. They are the Ohm conductive particle (Section 2, Subsection 2.4), the Debye model of polar dielectric (Subsection 3.3), and the Lorentz model of non-polar dielectric (Subsection 3.4). Models can be complicated and combined. The particles with hybrid conductor-dielectric properties are considered in Section 4. All the models are supported by corresponding numerical examples in Subsections 2.5, 3.3.1, 3.4.1 and 4.1.

Conclusion and a possible application of presented results in the particle trap physics is discussed in Section 5.

All analytical calculations are presented in the CGS system. Some input and output data in the numerical examples are given in commonly used non-CGS units.

## 2 Spherical conductive particle rotating in the uniform electrostatic field

### 2.1 Electrostatics of a rotating conductor

Let us consider an electrically neutral rigid particle rotating in vacuum. The particle consists of a uniform conducting medium of the volume charge density  $\rho$  and the current density  $\mathbf{j}$  in the laboratory reference frame. We are interested of an electric response of the particle on an external uniform electrostatic field, i.e., the charge redistribution and the local electric field inside and around the particle. We suppose that relativistic effects are negligible. Thus one can apply the set of quasi-static electric field equations [1, Table I] to our case of the rotating conductor.

We describe the rotary motion of the particle by means of the time-dependent matrix  $\mathbf{O}(t) \in \text{SO}(3)$ :  $\mathbf{r}' = \mathbf{O}(t)\mathbf{r}(t)$ , where  $\mathbf{r}(t)$  is a radius-vector of any material point of particle in the laboratory reference frame, and  $\mathbf{r}'$  is a corresponding constant vector in the proper reference frame (where the particle is motionless). We will assume that in the proper reference frame the electric field  $\mathbf{E}' = \mathbf{O}\mathbf{E}$  and the current density  $\mathbf{j}'$  are related by the local Ohm law:

$$\mathbf{j}' = \varkappa\mathbf{E}', \quad (2.1)$$

where the conductivity  $\varkappa$  is a positive constant. Then in the laboratory reference frame the current density includes the conduction part and the convection part [1]:

$$\mathbf{j} = \varkappa\mathbf{E} + \rho\mathbf{v} \quad (2.2)$$

where

$$\mathbf{v} = -\mathbf{O}^T\dot{\mathbf{O}}\mathbf{r} = \boldsymbol{\Omega} \times \mathbf{r} \quad (2.3)$$

is the velocity of the point  $\mathbf{r}$ ,  $\dot{\mathbf{O}} \equiv d\mathbf{O}/dt$ , the angular velocity vector  $\boldsymbol{\Omega}$  is dual to the skew-symmetric matrix  $\mathbf{O}^T\dot{\mathbf{O}}$ , and “ $\times$ ” denotes the cross product of vectors.

We suppose that despite of rotation the particle is in a steady state, at least adiabatically (this term will be clarified farther). Thus

$$\partial\rho/\partial t = 0 \quad \implies \quad \nabla \cdot \mathbf{j} = 0, \quad (2.4)$$

and the equations for the electrostatic potential  $\varphi$  hold:

$$\mathbf{E} = -\nabla\varphi, \quad (2.5a)$$

$$\nabla \cdot \mathbf{E} = -\Delta\varphi = 4\pi\rho. \quad (2.5b)$$

The equations (2.2)–(2.5) yield the equation for the charge density in the bulk of particle:

$$\boldsymbol{\Omega} \cdot (\mathbf{r} \times \nabla)\rho + 4\pi\kappa\rho = 0. \quad (2.6)$$

The bulk equations (2.4)–(2.6) are complemented with the boundary conditions:

$$E_n^+ - E_n^- = 4\pi\sigma, \quad (2.7)$$

$$\varphi^+ - \varphi^- = 0, \quad (2.8)$$

$$\nabla \cdot \mathbf{i} - j_n^- = 0; \quad (2.9)$$

here  $\sigma$  and  $\mathbf{i}$  are the charge and the current surface densities, the superscript “–” denotes the surface approach from the internal medium side, the superscript “+” denotes the approach from the external vacuum side, and the unit normal  $\mathbf{n}$  is directed outside the particle surface so that  $j_n^+ \equiv \mathbf{n} \cdot \mathbf{j}^+ = 0$ .

## 2.2 Charge balance equations

We consider a spherical particle of the radius  $R$  and the conductivity  $\kappa$  rotating with the constant angular velocity  $\boldsymbol{\Omega}$  in the external uniform electrostatic field. We denote this field by the constant vector  $\boldsymbol{\mathcal{E}}$  to distinguish from the aforementioned local electric field  $\mathbf{E}$ . Let  $\boldsymbol{\Omega}$  be directed along the orth  $\mathbf{e}_z$  of the Cartesian coordinate system  $Oxyz$  in the laboratory reference frame, i.e.,  $\boldsymbol{\Omega} = \Omega \mathbf{e}_z$ . This can be done by the following choice of the matrix  $\mathbf{O}(t) \in \text{SO}(3)$ :

$$\mathbf{O}(t) = \begin{bmatrix} \cos \Omega t & \sin \Omega t & 0 \\ -\sin \Omega t & \cos \Omega t & 0 \\ 0 & 0 & 1 \end{bmatrix}. \quad (2.10)$$

Then we use the spherical coordinate system built from the center of the particle,

$$\begin{aligned} x &= r \sin \theta \cos \alpha, & y &= r \sin \theta \sin \alpha, & z &= r \cos \theta, \\ 0 &\leq r < \infty, & 0 &\leq \theta \leq \pi, & 0 &\leq \alpha < 2\pi \end{aligned} \quad (2.11)$$

and endowed by the right orth triplet  $\mathbf{e}_r, \mathbf{e}_\theta, \mathbf{e}_\alpha$  at every point  $\mathbf{r}$ ; Fig. 1.

Then the equation (2.6) takes the form

$$\Omega \partial\rho/\partial\alpha + 4\pi\kappa\rho = 0, \quad (2.12)$$

and the only continuous solution is  $\rho = 0$ , as in the static case  $\Omega = 0$ . Nevertheless, the charge can accrue in the surface layer of some small thickness  $h$  yielding the surface density  $\sigma = h\rho|_{r=R}$ .

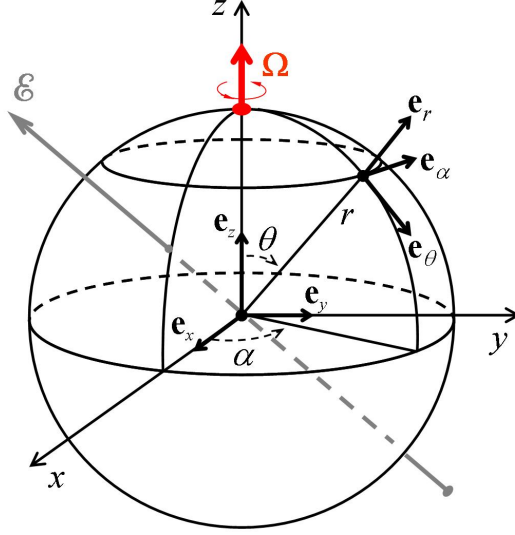


Figure 1: The choice of the spherical coordinate system convenient to derive the polarization of a rotating particle in the uniform electric field  $\mathbf{E}$ .

In contrast, the current can flow along both the bulk and surface, so that

$$\mathbf{j} = j_r \mathbf{e}_r + j_\theta \mathbf{e}_\theta + j_\alpha \mathbf{e}_\alpha = \varkappa \mathbf{E}, \quad (2.13)$$

$$\mathbf{i} \equiv h \mathbf{j}|_{r=R} = i_\theta \mathbf{e}_\theta + i_\alpha \mathbf{e}_\alpha = [\kappa \mathbf{E}_T + \sigma \boldsymbol{\Omega} \times \mathbf{r}]_{r=R}, \quad (2.14)$$

where  $\mathbf{i}$  is a surface current density,  $\mathbf{E}_T \equiv \mathbf{E} - E_n \mathbf{n} = E_\theta \mathbf{e}_\theta + E_\alpha \mathbf{e}_\alpha$  is the tangential projection of  $\mathbf{E}$  to the particle surface, and  $\kappa \equiv h \varkappa$ ; but one can assume in general  $\kappa \neq h \varkappa$  if electric properties of the surface layer differ from the bulk ones. For example, one can put  $\varkappa R \lesssim \kappa$  if a poor-conducting particle is covered with the well-conducting layer, or  $\varkappa = 0$  if the core is dielectric. This example will be considered in the Section 4, Subsection 4.1.2.

The charge conservation law (2.4) is fulfilled in the bulk by the equations (2.2), (2.5b) with  $\rho = 0$  in r.-h.s. For the surface layer one should write down the boundary condition (2.9) in spherical coordinates. It is illustrative to treat (2.9) as an application of the conservation law (2.4) in the integral form, where the integration runs over a surface of a small volume segment of the layer; Fig. 2:

$$\oint d\mathbf{s} \cdot \mathbf{j} = -j_r ab + [\tilde{b} j_{\theta+\delta\theta} - b j_\theta] h + [j_{\alpha+\delta\alpha} - j_\alpha] ha = 0, \quad (2.15)$$

where  $a = R\delta\theta$ ,  $b = R \sin \theta \delta\alpha$ ,  $\tilde{b} = R \sin(\theta + \delta\theta) \delta\alpha$ , and  $h$  is a thickness of the layer. One arrives at the equation:

$$\frac{\partial(i_\theta \sin \theta)}{\partial \theta} + \frac{\partial i_\alpha}{\partial \alpha} - R j_r^- \sin \theta = 0 \quad (2.16)$$

where  $j_r^-$  is the radial component of the volume current density just below the surface layer.

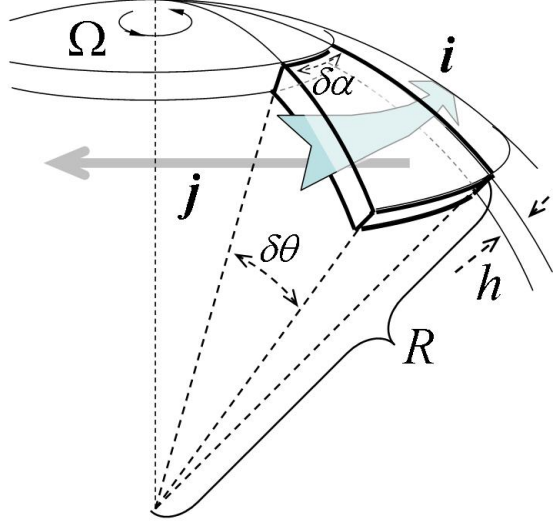


Figure 2: Current balance in a surface layer of the rotating particle; visualization of the equations (2.13)–(2.16)

### 2.3 Electrostatic potential

Up to this point a solution of the electrostatic equations (2.5) and boundary conditions (2.7), (2.8) including the surface charge density  $\sigma$  remained unknown. From now on we imply the surface layer negligibly thin,  $h \rightarrow 0$ , and use the following ansatz for the electrostatic potential:

$$\varphi = -\boldsymbol{\mathcal{E}} \cdot \boldsymbol{r} + \frac{R^3}{r^3} \boldsymbol{\mathcal{P}} \cdot \boldsymbol{r}, \quad r > R, \quad (2.17a)$$

$$\varphi = -(\boldsymbol{\mathcal{E}} - \boldsymbol{\mathcal{P}}) \cdot \boldsymbol{r}, \quad r < R, \quad (2.17b)$$

where  $\boldsymbol{\mathcal{P}}$  is an unknown constant vector to be found. This potential satisfies the boundary condition (2.8). The 1st term in r.-h.s of (2.17a) is the potential of the external field  $\boldsymbol{\mathcal{E}}$ , and the 2nd one is the potential of the dipole moment  $\boldsymbol{d} = R^3 \boldsymbol{\mathcal{P}}$ . Was  $\boldsymbol{\mathcal{P}} = \boldsymbol{\mathcal{E}}$ , one arrives at the static case  $\Omega = 0$ .

It follows from (2.17) the field on the surface:

$$\begin{aligned} \boldsymbol{E}^+ &\equiv \boldsymbol{E}|_{r \rightarrow R+0} = \boldsymbol{\mathcal{E}} - \boldsymbol{\mathcal{P}} + 3\mathcal{P}_r \boldsymbol{e}_r, \\ \boldsymbol{E}^- &\equiv \boldsymbol{E}|_{r \rightarrow R-0} = \boldsymbol{\mathcal{E}} - \boldsymbol{\mathcal{P}}, \end{aligned}$$

then the boundary condition (2.7) yields the surface charge density:

$$\sigma = \frac{1}{4\pi} (E_r^+ - E_r^-) = \frac{3}{4\pi} \mathcal{P}_r. \quad (2.18)$$

Relations (2.11) between Cartesian and spherical coordinates yield relations between

corresponding vector components, for one:

$$\begin{aligned}
\boldsymbol{\mathcal{E}} &= \mathcal{E}_x \mathbf{e}_x + \mathcal{E}_y \mathbf{e}_y + \mathcal{E}_z \mathbf{e}_z \equiv \mathcal{E}_r \mathbf{e}_r + \mathcal{E}_\theta \mathbf{e}_\theta + \mathcal{E}_\alpha \mathbf{e}_\alpha \\
&= (\mathcal{E}_x \sin \theta \cos \alpha + \mathcal{E}_y \sin \theta \sin \alpha + \mathcal{E}_z \cos \theta) \mathbf{e}_r \\
&\quad + (\mathcal{E}_x \cos \theta \cos \alpha + \mathcal{E}_y \cos \theta \sin \alpha - \mathcal{E}_z \sin \theta) \mathbf{e}_\theta \\
&\quad\quad + (-\mathcal{E}_x \sin \alpha + \mathcal{E}_y \cos \alpha) \mathbf{e}_\alpha
\end{aligned} \tag{2.19}$$

etc. Gathering all expressions involved in (2.13)–(2.14) and then requiring the equality (2.16) at every point of the surface, one arrives at the set of equations for components of the vector  $\mathcal{P}$ :

$$\begin{aligned}
(\varkappa + 2\kappa/R) (\mathcal{E}_x - \mathcal{P}_x) &= \frac{3\Omega}{4\pi} \mathcal{P}_y, \\
(\varkappa + 2\kappa/R) (\mathcal{E}_y - \mathcal{P}_y) &= -\frac{3\Omega}{4\pi} \mathcal{P}_x, \\
\mathcal{E}_z - \mathcal{P}_z &= 0.
\end{aligned} \tag{2.20}$$

In view of the spherical symmetry of the problem one can put  $\mathcal{E}_y = 0$  without loss of generality. Then the solution of the set (2.20) is

$$\mathcal{P}_x = \frac{\mathcal{E}_x}{1 + \tau_0^2 \Omega^2}, \quad \mathcal{P}_y = \frac{\tau_0 \Omega \mathcal{E}_x}{1 + \tau_0^2 \Omega^2}, \quad \mathcal{P}_z = \mathcal{E}_z, \tag{2.21}$$

where

$$\tau_0 = \frac{3}{4\pi(\varkappa + 2\kappa/R)} \tag{2.22}$$

is the characteristic time scale, during which the charge distribution follows the change of the particle orientation with respect to the external field. In particular,  $\mathcal{P} \xrightarrow[\Omega \rightarrow 0]{} \boldsymbol{\mathcal{E}}$ , as it is expected in the static case, so the field inside the conducting sphere disappears,  $\mathbf{E} = 0$ . On the other hand,  $\mathcal{P}_x \xrightarrow[\Omega \rightarrow \infty]{} 0$ ,  $\mathcal{P}_y \xrightarrow[\Omega \rightarrow \infty]{} 0$ , i.e., the charge distribution cannot follow a fast rotation and smears over the surface.

It is convenient to represent the solution (2.21) in coordinateless form. For this purpose we recall the definition of the Cartesian orth triplet according to Fig. 1:

$$\begin{aligned}
\boldsymbol{\Omega} \parallel \mathbf{e}_z &\implies \mathbf{e}_z = \boldsymbol{\Omega}/\Omega, \quad \text{where } \Omega = |\boldsymbol{\Omega}|; \\
\boldsymbol{\mathcal{E}} \in Oxz &\implies \mathbf{e}_x = \boldsymbol{\mathcal{E}}_\perp/\mathcal{E}_\perp, \quad \text{where } \boldsymbol{\mathcal{E}}_\perp = \boldsymbol{\mathcal{E}} - (\boldsymbol{\mathcal{E}} \cdot \boldsymbol{\Omega})\boldsymbol{\Omega}/\Omega^2 \\
&\quad \mathbf{e}_y = \mathbf{e}_z \times \mathbf{e}_x.
\end{aligned} \tag{2.23}$$

Then, using (2.21) and (2.23) we have:

$$\mathcal{P} = \mathcal{P}_x \mathbf{e}_x + \mathcal{P}_y \mathbf{e}_y + \mathcal{P}_z \mathbf{e}_z = \frac{1}{1 + \tau_0^2 \Omega^2} \{ \boldsymbol{\mathcal{E}} + \tau_0 \boldsymbol{\Omega} \times \boldsymbol{\mathcal{E}} + \tau_0^2 (\boldsymbol{\Omega} \cdot \boldsymbol{\mathcal{E}}) \boldsymbol{\Omega} \}. \tag{2.24}$$

Equations (2.17), (2.24) represent 3D generalization of the 2D electrostatic potential known for the particular case  $\boldsymbol{\mathcal{E}} \perp \boldsymbol{\Omega}$  [2,3] and used for a description of the Quincke effect.

## 2.4 Rotary dynamics

It follows from the previous section that the spherical conductor rotating in the static uniform electric field acquires the dipole moment  $\mathbf{d} = R^3\mathcal{P}$  which interaction with the external field  $\mathcal{E}$  changes the angular momentum of the particle as follows

$$I \frac{d\boldsymbol{\Omega}}{dt} = \mathbf{M} \equiv \mathbf{d} \times \mathcal{E} = R^3\mathcal{P} \times \mathcal{E}, \quad (2.25)$$

where  $I$  is the inertia moment of the spherical particle. The equation is somewhat inconsistent since the solution (2.17), (2.24) was built for a steady state configuration, provided  $\mathcal{E}$ ,  $\boldsymbol{\Omega}$  and thus  $\mathcal{P}$  are constant vectors. Actually, we adopt the adiabatic approximation, i.e., we assume that the charge and current distributions follow immediately or very quickly the change of the angular velocity  $\boldsymbol{\Omega}(t)$ , i.e., the vector  $\mathcal{P}(t) = \mathcal{P}[\boldsymbol{\Omega}(t)]$ .

Inserting this expression into the equation (2.25) reduces the latter to the form of non-linear Euler equation:

$$I \frac{d\boldsymbol{\Omega}}{dt} = \frac{\tau_0 R^3}{1 + \tau_0^2 \Omega^2} \mathcal{E} \times \{ \mathcal{E} \times \boldsymbol{\Omega} - \tau_0 (\boldsymbol{\Omega} \cdot \mathcal{E}) \boldsymbol{\Omega} \}. \quad (2.26)$$

It is convenient to split this vector equation by means of new Cartesian coordinate system spanned on the orth triplet  $\mathbf{e}_1, \mathbf{e}_2, \mathbf{e}_3$  such that  $\mathcal{E} = \mathcal{E}\mathbf{e}_3$ ; Fig. 3.

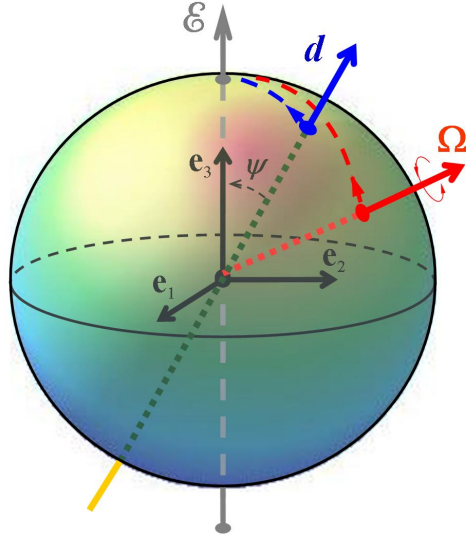


Figure 3: The choice of the Cartesian coordinate system convenient to describe a rotary dynamics of the particle in the uniform electric field  $\mathcal{E}$ .

Introducing dimensionless variables:

$$\boldsymbol{\omega} = \tau_0 \boldsymbol{\Omega}, \quad \tau = t/T_0, \quad (2.27)$$

where the time scale parameter  $\tau_0$  is defined by (2.22), and

$$T_0 = I/(\tau_0 R^3 \mathcal{E}^2), \quad (2.28)$$

reduces (2.26) to the dimensionless component set:

$$\frac{d\omega_1}{d\tau} = -\frac{\omega_1 - \omega_3\omega_2}{1 + \omega^2}, \quad (2.29)$$

$$\frac{d\omega_2}{d\tau} = -\frac{\omega_2 + \omega_3\omega_1}{1 + \omega^2}, \quad (2.30)$$

$$\frac{d\omega_3}{d\tau} = 0. \quad (2.31)$$

Thus  $\omega_3 = \text{const}$ , and the vector  $\boldsymbol{\omega}_\perp \equiv \{\omega_1, \omega_2, 0\}$  is to be found.

Adding (2.29) multiplied by  $\omega_1$  with (2.30) multiplied by  $\omega_2$  yields the equation for  $\omega_\perp^2 \equiv \boldsymbol{\omega}_\perp \cdot \boldsymbol{\omega}_\perp = \omega_1^2 + \omega_2^2$ :

$$\frac{d\omega_\perp^2}{d\tau} = -\frac{2\omega_\perp^2}{1 + \omega_3^2 + \omega_\perp^2}$$

which integration results in the formula:

$$\ln \nu + \nu = \ln \nu_0 + \nu_0 - 2\tau/\xi, \quad (2.32)$$

where

$$\nu \equiv \omega_\perp^2/\xi, \quad \xi = 1 + \omega_3^2, \quad \nu_0 = \nu|_{\tau=0}.$$

This implicit dependency of  $\omega_\perp^2$  on  $\tau$  can be presented explicitly by means of the Lambert W-function [7]:

$$\nu = W_0(\nu_0 e^{\nu_0 - 2\tau/\xi}). \quad (2.33)$$

Now introducing the subsidiary evolution parameter

$$\lambda = \ln \sqrt{\nu_0/\nu}, \quad \lambda \sim \frac{\tau}{1 + \omega_3^2} \quad \text{at} \quad \tau \rightarrow \infty \quad (2.34)$$

reduces the set (2.29)-(2.30) to the linear equations with constant coefficients:

$$\begin{aligned} d\omega_1/d\lambda &= -\omega_1 - \omega_3\omega_2, \\ d\omega_2/d\lambda &= -\omega_2 + \omega_3\omega_1, \end{aligned}$$

which solution reads:

$$\omega_1 = \omega_{10} e^{-\lambda} \cos \phi, \quad \omega_2 = \omega_{10} e^{-\lambda} \sin \phi, \quad \phi = -\omega_3 \lambda. \quad (2.35)$$

Here, using the spherical symmetry, we put  $\omega_{20} \equiv \omega_2(0) = 0$  so that  $\omega_{10} = |\omega_{10}|$ .

The vector  $\boldsymbol{\mathcal{P}}$  and thus the dipole moment  $\boldsymbol{d}$  are inclined to the direction  $\boldsymbol{e}_3$  of the vector  $\boldsymbol{\mathcal{E}}$  by the angle  $\psi$  (see Figure 3):

$$\tan \psi = \omega_\perp / \sqrt{1 + \omega_3^2} \quad (2.36)$$

which is maximal if  $\omega_3 = 0$ .

Coming back to the dimensional variables, let us present the solution (2.35) asymptotically, at  $t \rightarrow \infty$ :

$$\Omega_\perp \sim e^{-t/T}, \quad \phi \sim -\tilde{\Omega}_3 t, \quad (2.37)$$

where

$$T = T_0(1 + \tau_0^2 \Omega_3^2), \quad \tilde{\Omega}_3 = \Omega_3 \tau_0 / T. \quad (2.38)$$

It follows from (2.37) that the transversal to  $\boldsymbol{\mathcal{E}}$  component  $\boldsymbol{\Omega}_\perp$  of the angular velocity  $\boldsymbol{\Omega}$  decreases in its magnitude exponentially with the braking time  $T$  and precesses clockwise with the angular velocity  $\tilde{\Omega}_3$ . The inclination angle  $\psi \rightarrow 0$  by the same exponential law.

## 2.5 Numerical examples

If the spherical particle is homogeneous the mass and the inertia moment are:

$$m = \frac{4}{3}\pi\mu R^3, \quad I = \frac{2}{5}mR^2 = \frac{8}{15}\pi\mu R^5$$

where  $\mu$  is a mass density. Besides, the surface conductivity is negligible compared to the effect of the bulk one:  $\kappa/(\varkappa R) = h/R \rightarrow 0$ . Then two time scale parameters (2.22) and (2.28) present in the problem specify as follows:

$$\tau_0 = \frac{3}{4\pi\varkappa}, \quad T_0 = \frac{32\pi^2}{45} \frac{\mu\varkappa R^2}{\mathcal{E}^2}.$$

The first one does not depend on the size of particle. It determines the relaxation time in which the charge distribution of the particle follows its rotary motion. The second scale parameter, actually, is  $T = T_0(1 + \tau_0^2\Omega_3^2)$ ; it determines the characteristic time in which  $\Omega_\perp \rightarrow 0$ , as it follows from (2.37). The approach of the vector  $\mathbf{\Omega}_\perp \rightarrow 0$  and thus  $\mathcal{P} \rightarrow \mathcal{E}$  is accompanied by a precession with the angular velocity  $\tilde{\Omega}_3 = \Omega_3\tau_0/T$ , as it follows from the solution (2.35), (2.34) or (2.37), (2.38).

Let us recall that this solution corresponds to the adiabatic approximation which in present case is valid provided  $\tau_0 \ll T$ .

Here we consider two examples of metallic particles: the golden particle (the perfect conductor) and the nichrome particle (higher resistance conductor). In these and subsequent examples the size and the maximal angular velocity will be put as in the experiment [4]:  $R = 50$  nm,  $\Omega_{\max} = 2\pi$  GHz. We put the external field  $\mathcal{E} = 33.4$  statV/cm (i.e.,  $10^6$  V/m in SI units) which is characteristic for devices like the Van der Graaf electrostatic generator e.t.c. This value provides an essential induced dipole moment of conductive particles  $d \approx R^3\mathcal{E} \approx 4400$  Debyes =  $4.4 \cdot 10^{-15}$  statC·cm, the same value as the permanent dipole moment of the polar cellulose nanocrystals [8].

### 2.5.1 Perfect conductor: golden nanoparticle

$\mu = 19.31$  g/cm<sup>3</sup>,  $\varkappa = 36.9 \cdot 10^{16}$  s<sup>-1</sup> (i.e.,  $4.1 \cdot 10^7$  S/m in SI). Then  $\tau_0 = 6.37 \cdot 10^{-19}$  s, and  $\omega \leq \omega_{\max} = \tau_0\Omega_{\max} = 4 \cdot 10^{-9}$ . Thus the braking time  $T \approx T_0 = 1.14 \cdot 10^6$  s  $\approx 13$  days is of order of a storage time in Penning trap [9]. Since  $T \gg \tau_0$ , the adiabatic approximation is perfect. The initial inclination angle is not more than  $\psi \lesssim 4 \cdot 10^{-9}$ , so the effect is negligible.

### 2.5.2 High resistance conductor: nichrome nanoparticle

$\mu = 8.5$  g/cm<sup>3</sup>,  $\varkappa = 9 \cdot 10^{15}$  s<sup>-1</sup> (i.e.,  $10^6$  S/m in SI). Then  $\tau_0 = 2.66 \cdot 10^{-17}$  s, and  $\omega \leq \tau_0\Omega_{\max} = 1,7 \cdot 10^{-7}$ . Thus the inclination is negligible,  $\psi \lesssim 1.7 \cdot 10^{-7}$ , and  $T \approx T_0 = 1.2 \cdot 10^4$  s  $\approx 3.34$  hours. Again,  $T \gg \tau_0$ , and the adiabatic approximation is perfect.

### 3 Spherical dielectric particle rotating in the uniform electrostatic field

#### 3.1 Electrostatics of a rotating dielectric

We assume that in the proper reference frame the material equation relating the electric field  $\mathbf{E}'$  and the electric induction  $\mathbf{D}'$  is linear, isotropic but time-nonlocal:

$$\mathbf{D}'(t) = \int_{-\infty}^t dt' \epsilon(t-t') \mathbf{E}'(t'). \quad (3.1)$$

The transition to the laboratory reference frame,  $\mathbf{E}'(t) = \mathbf{O}(t)\mathbf{E}$ , where the electric field  $\mathbf{E}$  is again assumed static, yields thus the static but anisotropic relation:

$$\mathbf{D} = \hat{\epsilon}\mathbf{E}, \quad (3.2)$$

where the tensor of dielectric permittivity

$$\hat{\epsilon} = \int_0^{\infty} dt \epsilon(t) \mathbf{O}^T(t), \quad (3.3)$$

is determined via the kernel  $\epsilon(t)$  and the rotation matrix (2.10) transposed  $\mathbf{O}^T(t)$ . Explicitly,

$$\hat{\epsilon} = \begin{bmatrix} \epsilon_r & -\epsilon_i & 0 \\ \epsilon_i & \epsilon_r & 0 \\ 0 & 0 & \epsilon_s \end{bmatrix}, \quad (3.4)$$

where

$$\epsilon_r \equiv \text{Re } \epsilon(\Omega), \quad \epsilon_i \equiv \text{Im } \epsilon(\Omega), \quad \epsilon_s \equiv \epsilon(0), \quad \epsilon(\Omega) \equiv \int_0^{\infty} dt \epsilon(t) e^{i\Omega t}, \quad (3.5)$$

$\text{Re } \epsilon(\Omega)$  and  $\text{Im } \epsilon(\Omega)$  are the real and imaginary parts of the dielectric function  $\epsilon(\Omega)$  to be the Fourier transform of the kernel  $\epsilon(t)$ , and  $\epsilon_s$  is the static dielectric constant.

We will use the same ansatz (2.17) for the electrostatic potential with the polarization vector  $\mathcal{P}$  to be found, but the boundary condition (2.7) will be reformulated in terms of the electric induction field:

$$E_r^+ = D_r^-. \quad (3.6)$$

Using the expansions like (2.19) one can recast the condition (3.6) into the following equation for the polarization vector  $\mathcal{P}$ :

$$\mathcal{E} + 2\mathcal{P} = \hat{\epsilon}(\mathcal{E} - \mathcal{P})$$

which can be solved in the symbolic form:

$$\mathcal{P} = [\hat{\epsilon} + 2]^{-1}(\hat{\epsilon} - 1)\mathcal{E} \quad (3.7)$$

revealing the matrix analogue of the Clausius-Mossotti relation.

Using the spherical symmetry and putting (as before)  $\mathcal{E}_y = 0$ , one arrives at the explicit expressions:

$$\mathcal{P}_x = \frac{(\epsilon_r + 2)(\epsilon_r - 1) + \epsilon_i^2}{(\epsilon_r + 2)^2 + \epsilon_i^2} \mathcal{E}_x, \quad \mathcal{P}_y = \frac{3\epsilon_i}{(\epsilon_r + 2)^2 + \epsilon_i^2} \mathcal{E}_x, \quad \mathcal{P}_z = \frac{\epsilon_s - 1}{\epsilon_s + 2} \mathcal{E}_z. \quad (3.8)$$

### 3.2 Rotary dynamics

Combining the formulae (3.8) with the Cartesian orth triplet (2.23) and inserting the dipole moment  $\mathbf{d} = R^3 \mathcal{P}$  into the r.-h.s. of (2.25) one obtains the Euler equation

$$I \frac{d\boldsymbol{\Omega}}{dt} = \frac{R^3}{\Omega^2} \boldsymbol{\mathcal{E}} \times \left\{ \frac{3\varepsilon_i \Omega \boldsymbol{\mathcal{E}} \times \boldsymbol{\Omega}}{(\varepsilon_r + 2)^2 + \varepsilon_i^2} - \left[ \frac{\varepsilon_s - 1}{\varepsilon_s + 2} - \frac{(\varepsilon_r + 2)(\varepsilon_r - 1) + \varepsilon_i^2}{(\varepsilon_r + 2)^2 + \varepsilon_i^2} \right] (\boldsymbol{\Omega} \cdot \boldsymbol{\mathcal{E}}) \boldsymbol{\Omega} \right\}. \quad (3.9)$$

Choosing the dimensionless variables (2.27), (2.28), where  $\tau_0$  is some characteristic for a dielectric relaxation time (instead of (2.22) for a conductor), and splitting the Euler equation by components, we have again  $\omega_3 = \text{const}$ , and arrive at the set of nonlinear equations for  $\omega_1$  and  $\omega_2$ :

$$\begin{aligned} \frac{d\omega_1}{d\tau} &= -\frac{f(\omega^2)}{\omega^2} \omega_1 + \frac{g(0) - g(\omega^2)}{\omega^2} \omega_3 \omega_2, \\ \frac{d\omega_2}{d\tau} &= -\frac{f(\omega^2)}{\omega^2} \omega_2 - \frac{g(0) - g(\omega^2)}{\omega^2} \omega_3 \omega_1, \end{aligned} \quad (3.10)$$

where

$$f(\omega^2) = \frac{3\varepsilon_i \omega}{(\varepsilon_r + 2)^2 + \varepsilon_i^2} > 0, \quad g(\omega^2) = \frac{(\varepsilon_r + 2)(\varepsilon_r - 1) + \varepsilon_i^2}{(\varepsilon_r + 2)^2 + \varepsilon_i^2}.$$

The change of variables  $\omega_1, \omega_2 \mapsto \omega_\perp, \phi$ :

$$\omega_1 = \omega_\perp \cos \phi, \quad \omega_2 = \omega_\perp \sin \phi \quad (3.11)$$

reduces the set (3.10) to quadratures:

$$\tau = - \int \frac{d\omega_\perp^2 \omega^2}{2\omega_\perp^2 f(\omega^2)}, \quad (3.12)$$

$$\begin{aligned} \phi &= -\omega_3 \int d\tau \frac{g(0) - g(\omega^2)}{\omega^2} \\ &= \omega_3 \int \frac{d\omega_\perp^2 (g(0) - g(\omega^2))}{2\omega_\perp^2 f(\omega^2)}. \end{aligned} \quad (3.13)$$

The vector  $\mathcal{P}$  determining a particle polarization is inclined to the external field vector  $\boldsymbol{\mathcal{E}}$  by the angle  $\psi$  depending on the components of the angular velocity  $\boldsymbol{\omega}$ :

$$\tan^2 \psi = \frac{\{f^2(\omega^2)/\omega^2 + [g(0) - g(\omega^2)]^2 \omega_3^2\} \omega_\perp^2}{\{g(\omega^2) + [g(0) - g(\omega^2)] \omega_3\}^2}, \quad (3.14a)$$

$$\tan \psi \leq \tan \psi|_{\omega_3=0} = f(\omega^2)/g(\omega^2) \quad (3.14b)$$

since given  $\omega^2$ , the maximal value of  $\psi$  corresponds to  $\omega_3 = 0$ .

### 3.3 Debye relaxation model of polar dielectric

The simplest nontrivial form of the dielectric function arises from the Debye relaxation theory of polar dielectrics [10]. The material equation (3.1) in this case reads:

$$\mathbf{D}(t) = \mathbf{E}(t) + \int_{-\infty}^t dt' \chi(t-t') \mathbf{E}(t'), \quad (3.15)$$

where  $\chi(t) = \chi_0 e^{-t/\tau_0}$  and  $\tau_0$  is the relaxation time. With a commonly used minimal generalization [10,11] the corresponding dielectric function has the form:

$$\varepsilon(\Omega) = \varepsilon_\infty + \frac{\varepsilon_s - \varepsilon_\infty}{1 - i\tau_0\Omega}, \quad (3.16)$$

where  $\varepsilon_s = \varepsilon(0)$  is the static dielectric permittivity, and higher frequency absorption mechanisms are accounted by the phenomenological constant  $\varepsilon_\infty$ ; in general,  $\varepsilon_\infty \neq 1$ .

In terms of (2.27), (2.28), (3.5) we have:

$$\frac{\varepsilon_i}{\omega} = \frac{\varepsilon_s - \varepsilon_\infty}{1 + \omega^2}, \quad \varepsilon_r = \varepsilon_\infty + \frac{\varepsilon_i}{\omega}.$$

Inserting these functions into the quadratures (3.12), (3.13), one can derive the latter in the form:

$$-6(\varepsilon_s - \varepsilon_\infty)\tau = \{(\varepsilon_s + 2)^2 + (\varepsilon_\infty + 2)\omega_3^2\} \ln \omega_\perp^2 + (\varepsilon_\infty + 2)\omega_\perp^2; \quad (3.17)$$

$$\phi = \omega_3 \frac{\varepsilon_\infty + 2}{\varepsilon_s + 2} \ln \omega_\perp^2. \quad (3.18)$$

The change of the variable

$$\omega_\perp^2 \mapsto \nu = \frac{(\varepsilon_\infty + 2)^2}{3(\varepsilon_s - \varepsilon_\infty)\xi} \omega_\perp^2, \quad \text{where} \quad \xi = \frac{(\varepsilon_s + 2)^2 + (\varepsilon_\infty + 2)\omega_3^2}{3(\varepsilon_s - \varepsilon_\infty)}$$

reduces the solution (3.17) to the form (2.32), and then to the explicit one (2.33). Asymptotically, at  $t \rightarrow \infty$ , we have:

$$\Omega_\perp \sim e^{-t/T}, \quad \phi \sim -\frac{(\varepsilon_\infty + 2)\tau_0\Omega_3 t}{(\varepsilon_s + 2)T}, \quad (3.19)$$

where

$$T(\Omega_3) = \frac{8\pi}{45} \frac{(\varepsilon_s + 2)^2 + (\varepsilon_\infty + 2)^2\tau_0^2\Omega_3^2}{\varepsilon_s - \varepsilon_\infty} \frac{\mu R^2}{\tau_0 \mathcal{E}^2} \quad (3.20)$$

### 3.3.1 Numerical example: water ice

Going over to a numerical example, it is worth to note that the relaxation model (3.15) is appropriate for the description of polar liquids. Nevertheless, Debye shown [10] that the dielectric function (3.16) describes satisfactory a water ice, the polar solid. We consider here this example, using data from [10], corresponding to the ice temperature  $-2^\circ\text{C}$ :  $\mu = 0.9 \text{ g/cm}^3$ ,  $\varepsilon_s = 80$ ,  $\varepsilon_\infty = 2.2$ ,  $\tau_0 = 4.3 \cdot 10^{-5} \text{ s}$ .<sup>1</sup> Then for the record initial angular velocity  $\Omega_{\max} = 2\pi \cdot 10^9 \text{ s}^{-1}$  its dimensionless value  $\omega \leq \omega_{\max} = \tau_0\Omega_{\max} = 2.7 \cdot 10^5$ . Thus rotary effects are expected essential. Moreover, they depend strongly on the initial direction of  $\boldsymbol{\Omega}$  with respect to  $\boldsymbol{\mathcal{E}}$ , i.e., on the value of  $\omega_3 = \tau_0\Omega_3$ . In the case  $\omega_3 \approx \omega_{\max} = 2.7 \cdot 10^5$  the braking time  $T = 4.34 \cdot 10^{-2} \text{ s}$ , thus  $\tau_0 \ll T$  and the adiabatic approximation is appropriate. If  $\omega_3 \lesssim 1$ , the braking time decreases up to  $T = 2.3 \cdot 10^{-8} \text{ s}$ , and the validity of the adiabatic approximation becomes questionable. The initial inclination angle may approach  $\psi_{\max} \lesssim \pi/2$ , i.e., nearly  $\boldsymbol{\mathcal{P}} \perp \boldsymbol{\mathcal{E}}$ .

<sup>1</sup>This value of  $\tau_0$  is the indicated in [10] value of the settled life time of a molecule  $\tau_l = 2.2 \cdot 10^{-6} \text{ s}$  multiplied by the factor  $(\varepsilon_s + 2)/(\varepsilon_\infty + 2)$ .

The relaxation time of the *ice* appearing in the Debye dielectric function is unusually long compared to that of, say, *liquid water*,  $\tau_0 = 5 \cdot 10^{-10}$  s at 20°C [10]. If the water droplet rotates rigidly with the angular velocity  $\Omega \leq \Omega_{\max} = 2\pi \cdot 10^9$  s<sup>-1</sup>, the inclination angle  $\psi \lesssim 20^\circ$  is rather perceivable; it decreases in the braking time  $T \approx T_0 \approx 2 \cdot 10^{-3}$  s. But these figures are very approximate, since the deformation of the droplet by centrifugal and electrostatic forces is not taken into account.

The same or less order of the relaxation time  $\tau_0 \sim 10^{-11} - 10^{-12}$  s is characteristic for the polyvinyl chloride and some other polymer polar solids. But the Debye dielectric function (3.16) corresponding to the single relaxation time model is not appropriate for these cases, and phenomenological generalizations such as the Cole-Cole function or the Davidson-Cole function should be applied [11]. These dielectric functions are more complicated in calculations and are not considered in the present paper.

### 3.4 Lorentz oscillator model of non-polar dielectric

Following the Lorentz model [12] electrons in dielectrics are considered as the charged damped harmonic oscillators driven by the electric field penetrating in the dielectric. We consider the simplest single-resonant model based on the following dielectric function:

$$\varepsilon(\Omega) = \varepsilon_\infty + \frac{\Omega_p^2}{\Omega_0^2 - \Omega^2 - i\Gamma\Omega}, \quad (3.21)$$

where  $\Omega_p$  is the plasma frequency,  $\Omega_0$  is the resonance frequency,  $\Gamma$  is the damping decrement, and the value  $\varepsilon_\infty$  of the dielectric function at infinite frequency (instead of 1 in true Lorentz model) is used as an adjustable parameter for accounting higher frequency resonances.

Using the dimensionless variable and constants:

$$\omega = \Omega/\Omega_0, \quad \omega_p = \Omega_p/\Omega_0, \quad \gamma = \Gamma/\Omega_0, \quad (3.22)$$

we arrive at the relations for dielectric constants and functions:

$$\varepsilon_r = \varepsilon_\infty + \frac{(\varepsilon_s - \varepsilon_\infty)(1 - \omega^2)}{(1 - \omega^2)^2 + \gamma^2\omega^2}, \quad \frac{\varepsilon_i}{\omega} = \frac{\gamma^2(\varepsilon_s - \varepsilon_\infty)}{(1 - \omega^2)^2 + \gamma^2\omega^2}, \quad \varepsilon_s = \varepsilon_\infty + \omega_p^2.$$

Inserting these into the quadratures (3.12), (3.13), one derives those in the form:

$$\begin{aligned} -6\gamma(\varepsilon_s - \varepsilon_\infty)\tau = & \{[\varepsilon_s - \varepsilon_\infty + (\varepsilon_\infty + 2)(1 - \omega_3^2)]^2 + \gamma^2(\varepsilon_\infty + 2)^2\omega_3^2\} \ln \omega_\perp^2 \\ & - (\varepsilon_\infty + 2)\{2[\varepsilon_s - \varepsilon_\infty + (\varepsilon_\infty + 2)(1 - \omega_3^2)] - \gamma^2(\varepsilon_\infty + 2)\}\omega_\perp^2 \\ & + (\varepsilon_\infty + 2)^2\omega_\perp^4/2; \end{aligned} \quad (3.23)$$

$$-2\gamma(\varepsilon_s + 2)\phi = \omega_3\{[\varepsilon_s - \varepsilon_\infty + (\varepsilon_\infty + 2)(1 - \gamma^2 - \omega_3^2)] \ln \omega_\perp^2 - (\varepsilon_\infty + 2)\omega_\perp^2\}. \quad (3.24)$$

In contrast to pervious examples, this implicit solution cannot be unrevealed explicitly. Actually, one can explicit the asymptotical solution at  $\tau \rightarrow \infty$ :

$$\begin{aligned} \omega_\perp & \sim \exp \left\{ -\frac{3\gamma(\varepsilon_s - \varepsilon_\infty)\tau}{[\varepsilon_s - \varepsilon_\infty + (\varepsilon_\infty + 2)(1 - \omega_3^2)]^2 + \gamma^2(\varepsilon_\infty + 2)^2\omega_3^2} \right\}, \\ \phi & \sim 3\frac{\omega_3(\varepsilon_s - \varepsilon_\infty)[\varepsilon_s - \varepsilon_\infty + (\varepsilon_\infty + 2)(1 - \gamma^2 - \omega_3^2)]\tau}{[\varepsilon_s - \varepsilon_\infty + (\varepsilon_\infty + 2)(1 - \omega_3^2)]^2 + \gamma^2(\varepsilon_\infty + 2)^2\omega_3^2}. \end{aligned}$$

Even so, it is rather cumbersome. However, a practice corresponds mainly to the infrared domain  $\Omega/\Omega_0 \ll 1$  where the  $t \rightarrow \infty$  asymptotics simplifies considerably:

$$\Omega_{\perp} \sim e^{-t/T}, \quad \phi \sim \tilde{\Omega}_3 t, \quad (3.25)$$

$$\text{where } T = \frac{T_0(\varepsilon_{\infty} + 2)^2}{3(\varepsilon_s - \varepsilon_{\infty})}, \quad T_0 = \frac{I}{\tau_0 R^3 \mathcal{E}^2}, \quad \tau_0 = \frac{\Gamma}{\Omega_0^2}, \quad \tilde{\Omega}_3 = \frac{\Omega_3}{T\Gamma}. \quad (3.26)$$

In contrast to previous examples, here the precession is counterclockwise.

### 3.4.1 Numerical example: hexagonal silicon carbide

Following [13], dielectric properties of this material can be approximated satisfactory by the single resonant Lorentz function (3.21) with the parameters:  $\Omega_0 = 2\pi \cdot 23.8 \text{ THz} = 2\pi \cdot 2.38 \cdot 10^{13} \text{ s}^{-1}$ ,  $\omega_p^2 = \Omega_p^2/\Omega_0^2 = 3.305$ ,  $\gamma = \Gamma/\Omega_0 = 0.006$ ,  $\varepsilon_{\infty} = 6.7$ , so that  $\varepsilon_s = 10.005$ . Thus for even record frequency  $\Omega_{\max} = 2\pi \cdot 10^9 \text{ s}^{-1}$  the dimensionless value  $\omega \leq \omega_{\max} = \Omega_{\max}/\Omega_0 = 2.64 \cdot 10^{-4} \ll 1$ .

Taking into account the mass density  $\mu = 3.23 \text{ g/cm}^3$  and familiar for this work the external field  $\mathcal{E} = 33.4 \text{ statV/cm}$  one obtains  $\tau_0 = 2.5 \cdot 10^{-16} \text{ s}$ ,  $T = 7 \cdot 10^3 \text{ s} \approx 2 \text{ hours}$ , so that  $\tau_0 \ll T$ , and the adiabatic approximation is perfect. The time-scale quantity  $\tau_0$  is longer than that of conductors (even high resistance ones), but much shorter than the relaxation time of the ice. The braking time  $T$  and the inclination angle  $\psi \leq 4.8 \cdot 10^{-7}$  are close to those of nichrome.

## 4 Poor conductors and conductor-coated dielectrics

Results of previous subsections permit us to consider poor-conductor and non-homogeneous particles. We consider a very simple model of a poor-conductor particle or a dielectric core layered by the well-conducting shell. The high- and low-frequency properties of the core is characterized by the dielectric constant  $\varepsilon \equiv \varepsilon_{\infty}$  and the bulk conductivity  $\varkappa$ , respectively, while the shell of the thickness  $h \ll R$  (if any) possesses the surface conductivity  $\kappa$ . Dispersion of these quantities can be but here is not taken into account.

The ansatz for the potential (2.17) remains valid while the boundary condition (2.18) or (3.6) changes:

$$\sigma = \frac{1}{4\pi}(E_r^+ - D_r^-) = \frac{3}{4\pi}\tilde{\mathcal{P}}_r, \quad (4.1)$$

where  $\mathbf{D}^- = \varepsilon \mathbf{E}^-$  and

$$\tilde{\mathcal{P}} = [(\varepsilon + 2)\mathcal{P} - (\varepsilon - 1)\mathcal{E}]/3. \quad (4.2)$$

Subsequently, the components  $\mathcal{P}_y$  and  $\mathcal{P}_x$  in r.-h.s. of the equations (2.22) must be replaced formally by  $\tilde{\mathcal{P}}_y$  and  $\tilde{\mathcal{P}}_x$  which yields the solution:

$$\mathcal{P}_x = \frac{1 + \beta\tilde{\tau}_0^2\Omega^2}{1 + \tilde{\tau}_0^2\Omega^2} \mathcal{E}_x, \quad \mathcal{P}_y = \frac{(1 - \beta)\tilde{\tau}_0\Omega}{1 + \tilde{\tau}_0^2\Omega^2} \mathcal{E}_x, \quad \mathcal{P}_z = \mathcal{E}_z, \quad (4.3)$$

with

$$\tilde{\tau}_0 = \frac{\tau_0}{1 - \beta} = \frac{\varepsilon + 2}{4\pi(\varkappa + 2\kappa/R)}, \quad \beta = \frac{\varepsilon - 1}{\varepsilon + 2}, \quad (4.4)$$

instead of (2.21), (2.22). Then the torque in r.-h.s. of the Euler equation (2.25) or (2.26) must be replaced by the expression:

$$\mathbf{M} = \frac{(1-\beta)\tilde{\tau}_0 R^3}{1+\tilde{\tau}_0^2 \Omega^2} \boldsymbol{\varepsilon} \times \{\boldsymbol{\varepsilon} \times \boldsymbol{\Omega} - \tilde{\tau}_0(\boldsymbol{\Omega} \cdot \boldsymbol{\varepsilon})\boldsymbol{\Omega}\}. \quad (4.5)$$

The transition to the dimensionless variables

$$\boldsymbol{\omega} = \tilde{\tau}_0 \boldsymbol{\Omega}, \quad \tau = t/T_0,$$

where

$$T_0 = \frac{I}{(1-\beta)\tilde{\tau}_0 R^3 \mathcal{E}^2} = \frac{I}{\tilde{\tau}_0 R^3 \mathcal{E}^2},$$

reduces formally the Euler equation (2.25) to the same dimensionless component set (2.29)–(2.31). Let us note that the braking time is  $T = T_0(1 + \omega_3^2)$  where  $T_0$  does not depend on the dielectric permittivity of the core, but only on its and surface conductivity. The inclination angle is determined by the equation:

$$\tan \psi = \frac{(1-\beta)\sqrt{1+\omega_3^2}\omega_\perp}{|1+\beta\omega^2+(1-\beta)\omega_3|} \leq \tan \psi|_{\omega_3=0} = \frac{(1-\beta)\omega}{1+\beta\omega^2}.$$

## 4.1 Numerical examples

### 4.1.1 LISICON particle

Entrapment and study of levitating particles of solid electrolytes may appear useful for improving characteristics of these materials. Here we consider  $R = 50$  nm particles of the commonly used LISICON solid electrolyte [14,15]. Taking into account the mass density  $\mu = 2.8$  g/cm<sup>3</sup>, dielectric permittivity  $\varepsilon_\infty = 21.4$  and the conductivity  $\varkappa = 4.52 \cdot 10^{12}$  s<sup>-1</sup> (i.e., 502 S/m in SI) achieved in certain samples at temperature 250° C, one obtains the relaxation time  $\tilde{\tau}_0 = 4.1 \cdot 10^{-10}$  s. Since  $\omega \leq \tilde{\tau}_0 \Omega_{\max} = 2.6$ , rotary effects are not negligible. In particular, the inclination angle  $\psi \lesssim 2.8^\circ$ . The braking time  $T_0 = 0.002$  s  $\leq T_{\Omega_3 \approx \Omega_{\max}} = 0.015$  s, so the adiabatic approximation is reliable.

### 4.1.2 Gold-coated silica particle

Synthesis of silica nanoparticles covered by gold shell is currently elaborated [16,17] for physical, biological and medical use. We consider such a particle of the size  $R = 50$  nm (closed to those of [16]) with the fused silica core and the  $h = 3$  nm gold shell. Taking into account the mass density  $\mu = 2.2$  g/cm<sup>3</sup>, dielectric permittivity  $\varepsilon = 3.8$  and a practically zero conductivity of the fused silica, and corresponding data from Subsection 2.4 for the gold, one obtains the relaxation time  $\tilde{\tau}_0 = 10^{-17}$  s. Since  $\omega \leq \tilde{\tau}_0 \Omega_{\max} = 6.45 \cdot 10^{-8}$ , the braking time is  $T = T_0(1 + \tilde{\tau}_0^2 \Omega_3^2) \approx T_0 = 6.8 \cdot 10^5$  s  $\approx 13.3$  hours  $\gg \tilde{\tau}_0$ . Thus the adiabatic approximation is excellent while the inclination angle  $\psi \lesssim 6.45 \cdot 10^{-8}$  is tiny, similarly to the case of entirely golden particle.

## 5 Conclusion and application perspective

Free rotation of neutral spherical particles levitating in the uniform electrostatic field  $\boldsymbol{\varepsilon}$  has been considered. The external field  $\boldsymbol{\varepsilon}$  induces in particles the electric dipole moment

$\mathbf{d}$  which is inclined to this field due to particle rotation  $\mathbf{\Omega}$ . In turn, the interaction of the particle dipole moment  $\mathbf{d}$  with the external field  $\mathbf{E}$  causes the torque  $\mathbf{M} \equiv \mathbf{d} \times \mathbf{E}$  braking the particle rotation.

Three basic examples has been considered: the Ohm conductor, the Debye model of polar dielectric, and the Lorentz model of non-polar dielectric. Besides, the hybrid conductor-dielectric is also included. We assume that the distribution of free or bound charges resulting in a dipole moment follow adiabatically the change of particle rotation with the characteristic relaxation time  $\tau_0$ . The corresponding Euler equations of particle rotary motion are reduced to quadratures and integrated out. In all cases solutions reveal common features.

The parallel to the external field  $\mathbf{E}$  component of angular velocity is unchanged,  $\Omega_{\parallel} = \text{const}$ , while the orthogonal component  $\Omega_{\perp}$  decreases asymptotically (at  $t \rightarrow \infty$ ) by the exponential law  $\Omega_{\perp} \sim \exp\{-t/T\}$  with the characteristic braking time:

$$T(\Omega_{\parallel}) \geq T(0) \equiv T_0 \sim \frac{I}{\tau_0 R^3 \mathcal{E}^2} \sim \frac{\mu R^2}{\tau_0 \mathcal{E}^2}. \quad (5.1)$$

The same happens with the dipole moment:  $d_{\parallel} = \text{const}$  while  $d_{\perp} \sim \exp\{-t/T\}$ .

This behavior differs strongly from that of the Quincke effect in despite the electromechanical description of both cases is common. The difference is that the particle in our case is surrounded by vacuum while in Quincke's case it is immersed in a conducting viscous medium in which  $\Omega_{\parallel} = 0$  while  $\Omega_{\perp}$  and  $d_{\perp}$  are regarded as constants [1, 2]. Actually, the initial magnitude and direction of  $\mathbf{\Omega}$  can be arbitrary in both cases. But the viscous conducting medium dumps  $\Omega_{\parallel}$  quickly to zero and provides the particle polarization and corresponding torque opposite to that in our case. Consequently,  $\Omega_{\perp}$  evolves to non-zero asymptotical value at which the viscous torque compensates the electric one. This stationary state reached after transient processes is a stage of the Quincke effect, and its 2D description is sufficient.

In our case, namely the transition process of a particle 3D rotation is of interest since the estimated braking time in vacuum (5.1) may occur notable. At least,  $T \gg \tau_0$  for the adiabatic approximation to be valid. Details of this process depend on electric properties of particles.

The value of the relaxation time  $\tau_0$  varies in wide range, from  $\tau_0 \sim 6 \cdot 10^{-19}$  s for good conducting golden particles to  $\tau_0 \sim 5 \cdot 10^{-5}$  s for ice, the polar dielectric. The same is true for the maximal inclination angle at  $\Omega_{\text{max}} = 2\pi$  GHz: from  $\psi_{\text{max}} \sim 4 \cdot 10^{-9}$  to  $\psi_{\text{max}} \sim \pi/2$ . Ceteris paribus, the minimal braking time  $T_0$  is inversely proportional to the relaxation time  $\tau_0$ , thus it varies in wide range too: from  $T_0 \sim 10^6$  s for golden particles to  $T_0 \sim 2 \cdot 10^{-8}$  s for ice. Despite such a large difference in numbers, the solutions for Ohm conductors and Debye polar dielectrics are similar: up to a replacement of parameters, they coincide and can be represented in an explicit form via the Lambert W-function. In particular, they describe the clockwise precession with the angular velocity  $\tilde{\Omega}_{\parallel} \sim \Omega_{\parallel} \tau_0 / T$  of the vector  $\mathbf{\Omega}$  when turning to its asymptotical value  $\Omega_{\parallel} \mathbf{E} / \mathcal{E}$ .

In contrast, the simplest Lorentz model of non-polar dielectric characterized by the single resonance frequency  $\Omega_0$  leads to more complicated solution in implicit parametric form which describes the counterclockwise precession with the angular velocity  $\tilde{\Omega}_{\parallel} \sim \Omega_{\parallel} (T\Gamma)^{-1}$  in the infrared region  $\Omega < \Omega_0$ . The reason is that the real part  $\text{Re} \varepsilon(\Omega)$  of the Lorentz dielectric function (3.21) is increasing in this domain, in contrast to the Debye function (3.16).

Presented analytical solutions of the equations of rotary motion may have an application in the modern particle trap physics.

The motion of charged particles in the ideal Penning trap is described by an exact analytical solution of the corresponding equations of motion. This gives one possible to account imperfection effects as perturbations [18,19].

The capture of neutral particles is carried out using the interaction of their dipole moment with the electromagnetic field. For example, in the currently designed trap for neutral polar particles [20] the static sextupolar electric and quadrupolar magnetic confining fields are complemented by a strong uniform electric field intended to orient permanent dipole moments of particles along a symmetry axis of the device for better trapping. Equations of particle motion in this trap tangle translational and rotational degrees of freedom and are, in general, non-integrable.

The strong orientational electric field can be used not only for manipulating polar particles but also for inducing dipole moment in non-polar particles. The authors of the new design trap [20] consider the orientational electric field of order 0.1–1 V/m. But its strength is not restricted from above principally. Thus, a much stronger field can be assumed (in principle, up to the order of  $10^6$  V/m). Then namely this field in the first approximation will determine a rotary motion of particles while the confining fields can be accounted as perturbations. The problem raised in the present paper can be used to split approximately rotational degrees of freedom from translational ones and thus to simplify the analysis of the new design trap.

As it is noted above, the external electrostatic field suppresses, by dissipation, those components of the particle angular velocity which are transverse to the field. Therefore, the effect of the braking is not only the alignment of the induced dipole moment along the field, but also of the angular momentum of the particle, regardless of its initial rotation. For this, the particles do not necessarily have to levitate: the alignment can occur during the free fall of neutral particles in the field, if the braking time is small enough (as for some polar dielectrics or solid electrolytes). Therefore, the described effect may extend the perspectives of the aforementioned optomechanical experiments [4–6,21].

## References

- [1] G. I. Melcher, J. R. Taylor, Electrohydrodynamics: A review of the role of interfacial shear stresses, *Annual Review of Fluid Mechanics* 1 (1) (1969) 111–146. doi:10.1146/annurev.fl.01.010169.000551.
- [2] T. B. Jones, Quincke rotation of spheres, *IEEE Transactions of Industry Applications* IA-20 (4) (1984) 845–849. doi:10.1109/tia.1984.4504495.
- [3] T. B. Jones, *Electromechanics of particles*, Cambridge University Press, Cambridge, 1995.
- [4] R. Reimann, M. Doderer, E. Hebestrait, R. Diehl, M. Frimmer, D. Windey, F. Tebbenjohanns, L. Novotny, Ghz rotation of an optically trapped nanoparticle in vacuum, *Phys. Rev. Lett* 121 (3) (2018) 033602. doi:10.1103/PhysRevLett.121.033602.
- [5] J. Ahn, Z. Xu, J. Bang, P. Ju, X. Gao, T. Li, Ultrasensitive torque detection with an optically levitated nanorotor, *Nat. Nanotechnol.* 15 (2) (2020) 89–95. doi:10.1038/s41565-019-0605-9.

- [6] Y. Jin, J. Yan, S. J. Rahman, J. Li, X. Yu, J. Zhang, 6 GHz hyperfast rotation of an optically levitated nanoparticle in vacuum, *Photon. Res.* 9 (7) (2021) 1344–1350. doi:10.1364/PRJ.422975.
- [7] R. M. Corless, G. H. Gonnet, D. E. G. Hare, D. J. Jeffrey, D. E. Knuth, On the Lambert W function, *Adv. Comput. Math.* 5 (1) (1996) 329–359. doi:10.1007/BF02124750.
- [8] B. Frka-Petesic, B. Jean, L. Heux, First experimental evidence of a giant permanent electric-dipole moment in cellulose nanocrystals, *Europhys. Lett.* 107 (2) (2014) 28006. doi:10.1209/0295-5075/107/28006.
- [9] H. Häffner, T. Beier, S. Djekić, N. Hermanspahn, H.-J. Kluge, W. Quint, S. Stahl, J. Verdú, T. Valenzuela, G. Werth, Double Penning trap technique for precise  $g$  factor determinations in highly charged ions, *Eur. Phys. J. D* 22 (2) (2003) 163–182. doi:10.1140/epjd/e2003-00012-2.
- [10] P. J. W. Debye, *Polar Molecules*, Dover science books, Dover Publications, NY, 1929.
- [11] G. G. Raju, *Dielectrics in Electric Fields. Tables, Atoms, and Molecules*, 2nd Edition, CRC Press, Boca Raton, 2016. doi:10.1201/9781315373270.
- [12] H. A. Lorentz, *The Theory of Electrons: And its Applications to the Phenomena of Light and Radiant Heat*, 2nd Edition, Dover Publications, Inc., New York, 1952.
- [13] W. G. Spitzer, D. Kleinman, D. Walsh, Infrared properties of hexagonal silicon carbide, *Phys. Rev* 113 (1) (1959) 127–132. doi:10.1103/PhysRev.113.127.
- [14] D. Mazumdar, D. Bose, M. L. Mukherjee, Transport and dielectric properties of Lisicon, *Solid State Ionics* 14 (2) (1984) 143–147. doi:10.1016/0167-2738(84)90089-4.
- [15] L. Zhang, M. Malys, J. Jamroz, F. Krok, W. Wrobel, S. Hull, H. Yan, I. Abrahams, Structure and conductivity in LISICON analogues within the  $\text{Li}_4\text{GeO}_4\text{--Li}_2\text{MoO}_4$  system, *Inorg. Chem.* 62 (30) (2023) 11876–11886. doi:10.1021/acs.inorgchem.3c01222.
- [16] L. L. Felix, J. M. Porcel, F. F. H. Aragón, D. G. Pacheco-Salazar, M. H. Sousa, Simple synthesis of gold-decorated silica nanoparticles by in situ precipitation method with new plasmonic properties, *SN Appl. Sci.* 3 (4) (2021) 443. doi:10.1007/s42452-021-04456-0.
- [17] R. Trihan, O. Bogucki, A. Kozłowska, M. Ihle, S. Ziesche, B. Fetliński, B. Janaszek, M. Kieliszczyk, M. Kaczkan, F. Rossignol, A. Aimable, Hybrid gold-silica nanoparticles for plasmonic applications: A comparison study of synthesis methods for increasing gold coverage, *Heliyon* 9 (2023) e15977. doi:10.1016/j.heliyon.2023.e15977.
- [18] M. Vogel, *Particle confinement in Penning traps. An introduction*, Vol. 100 of Springer series on Atomic, Optical, and Plasma Physics, Springer, Cham, 2018.
- [19] Y. Yaremko, M. Przybylska, A. J. Maciejewski, Dynamics of a relativistic charge in the Penning trap, *Chaos* 25 (5) (2015) 053102. doi:10.1063/1.4919243.
- [20] M. Przybylska, A. J. Maciejewski, Yu. Yaremko, Electromagnetic trap for polar particles, *New J. Phys.* 22 (10) (2020) 103047. doi:10.1088/1367-2630/abb913.
- [21] H. Shi, M. Bhattacharya, Optomechanics based on angular momentum exchange between light and matter, *J. Physics B* 49 (15) (2016) 153001. doi:10.1088/0953-4075/49/15/153001.